The Journal of Experimental Biology 204, 4321–4334 (2001)
Printed in Great Britain © The Company of Biologists Limited 2001
JEB3630

Bimodal breathing in jumping spiders: morphometric partitioning of the lungs and tracheae in *Salticus scenicus* (Arachnida, Araneae, Salticidae)

Anke Schmitz* and Steven F. Perry

Institut für Zoologie, Rheinische Friedrich-Wilhelms-Universität Bonn, Poppelsdorfer Schloss, 53115 Bonn, Germany

*e-mail: ankeschmitz@uni-bonn.de

Accepted 5 October 2001

Summary

In jumping spiders, both the book lungs and the tracheal system are well-developed. The tracheal system consists of four thick primary tracheae that branch into small secondary tracheae, some of them ending in the opisthosoma and others entering the prosoma. We used stereological morphometric methods to investigate the morphological diffusing capacity of the lungs and of the walls of the secondary tracheae ('lateral diffusing capacity') of two groups of *Salticus scenicus* with mean body masses of 2.69 mg (group A) and 5.28 mg (group B). The thickness of the gas-exchange epithelium of the lungs was 0.164 μm (group A) and 0.186 μm (group B) for the total diffusion barrier. The secondary tracheae were divided arbitrarily into seven classes according to their inner diameter (1–7 μm). The diffusion barriers of the tracheal walls tend to be thinnest (0.17 and 0.18 μm) for the smallest tracheae, the walls of the other tracheal classes having approximately the same thickness of diffusion barrier (0.24–0.32 μm).

The calculated oxygen-diffusing capacity (D_{O_2}) for the lungs was 16.4 $\mu l\,min^{-1}\,g^{-1}\,kPa^{-1}$ for group A and 12 $\mu l\,min^{-1}\,g^{-1}\,kPa^{-1}$ for group B; the D_{O_2} of the walls of all secondary tracheae was 5.91 $\mu l\,min^{-1}\,g^{-1}\,kPa^{-1}$ for group A animals and 6.63 $\mu l\,min^{-1}\,g^{-1}\,kPa^{-1}$ for group B animals.

Our results are consistent with the hypothesis that the tracheal system plays an important role in gas exchange in jumping spiders. Resting and low-activity oxygen consumption rates can be met by the lungs or the tracheae alone, while high oxygen demands can be met only if both respiratory systems are working together. Tracheae entering the prosoma have only 4–10 % of the total tracheal diffusing capacity, thus providing sufficient oxygen for the nervous system but not being able to prevent muscle fatigue. The similar thickness of the walls of all tracheal classes is consistent with the hypothesis that the secondary tube tracheae function as 'tracheal lungs', supplying the haemolymph and organs by lateral diffusion.

Key words: Salticidae, jumping spider, *Salticus scenicus*, tracheal system, anatomical diffusing factor, lateral diffusing capacity, oxygen uptake, respiratory organ.

Introduction

Like most araneomorph spiders, jumping spiders possess a double respiratory system consisting of book lungs and tube tracheae. The book lungs are the most important for gas exchange in many species and cope alone with the oxygen demands. The tracheae are often only poorly developed and are presumed to be of little importance in overall gas exchange (Anderson, 1970; Anderson and Prestwich, 1982; Strazny and Perry, 1984). In contrast, several species, e.g. the diurnal jumping spiders, have both book lungs and tracheae that are well developed (Schmitz and Perry, 2000), but nothing is known about the gas-exchange potential of the tracheae in comparison with that of the lungs.

In *Salticus scenicus*, the tracheal system consists of four thick tube tracheae that originate from the atrium of the spiracle and that branch into secondary tracheae. These run parallel, without further branching, tapering slightly as they go. Some of the secondary tracheae end in the opisthosoma while others extend as bundles into the prosoma. Most tracheae end in the haemolymph; only the gut and the nervous system are penetrated in both the pro- and opisthosoma (Schmitz and Perry, 2000).

One way of describing the gas-exchange potential of a respiratory organ is to evaluate its morphological diffusing capacity. Quantitative morphological data on spider lungs have been obtained by counting the number of lung lamellae or interlamellar spaces and multiplying by the area of an average lamella (Anderson and Prestwich, 1980). Morphological diffusing capacities cannot, however, be calculated using this method. Only in *Tegenaria* spp. has the morphological diffusing capacity of the lungs been evaluated using stereological methods (Strazny and Perry, 1984). In addition, there is a lack of quantitative data on the surface areas, diffusion barriers and diffusing capacities of tracheal systems in spiders. Thus, evaluation of the functional morphology of tracheae, which initially involves identifying where gas exchange occurs, has been restricted to descriptive and speculative accounts. It is

known, however, that, in contrast to the insect tracheal system (Schmitz and Perry, 1999), the thickness of the tracheal walls in jumping spiders seems to be similar in all secondary tracheae (Schmitz and Perry, 2000), and the surface of all secondary tracheae could, therefore, play a role in gas exchange.

The circumstances leading to the evolution of tracheae within the Araneae are also poorly understood (Levi, 1967, 1976; Weygoldt and Paulus, 1979; Forster, 1980; Anderson and Prestwich, 1975). It has been suggested (i) that tracheae could provide better resistance to desiccation than lungs, (ii) that tracheae may be necessary when energy needs are increased (transition from 'sit-and-wait predator' to active predator) and (iii) that tracheae might provide important support for aerobic metabolism in the prosoma during periods of extended activity when prosomal pressures are high and haemolymph cannot be pumped from the opisthosoma against the pressure gradient.

In the present paper, we have evaluated the diffusing capacity of the lungs and of the secondary tracheae of *S. scenicus* using stereological morphometric methods and have compared these data with those from oxygen consumption measurements. These data enable us to test two hypotheses: (i) that the walls of all the secondary tracheae can serve as a gas-exchange surface, thus functioning as 'tracheal lungs', and (ii) that the tracheae constitute an important percentage of the total diffusing capacity of respiratory organs in jumping spiders and are essential for meeting high oxygen demands.

Materials and methods

Experimental animals and tissue processing

For stereological analysis, we examined two groups of jumping spiders (*Salticus scenicus*), each consisting of six female specimens, all caught in the vicinity of Bonn. Group A animals had a mean body mass (M_B) of 2.69±0.18 mg (mean ± S.D., range 2.55–2.8 mg, N=6) and group B animals had a mean M_B of 5.28±0.1 mg (range 5.1–5.5 mg, N=6).

The animals were weighed and cold-anaesthetised, and the legs, chelicerae and pedipalps were removed. The specimens were immediately transected between the prosoma and opisthososma and immersed in glutaraldehyde (3 % glutaraldehyde in 0.05 mol l^{-1} cacodylate buffer, pH 7.1; osmolarity 380–400 mosmol l^{-1}, 4 °C). The samples were fixed overnight, washed in buffer and postfixed with 1.5 % OsO_4 in the same buffer for 2 h at 0 °C. The samples were then dehydrated through an ethanol series and embedded in Epon 812. Semithin (0.5 μm) sections were prepared and stained with 0.05 % Toluidine Blue in 0.05 % borax. Ultrathin sections were prepared and contrasted with uranyl acetate and lead citrate before electron microscopic evaluation with a Zeiss EM 109.

Volume determination: Cavalieri principle on vertical sections

The volumes of the tracheal system and of the lungs were determined using the Cavalieri principle (Michel and Cruz-Orive, 1988), which estimates volume as the total cross-sectional area of sectioned material multiplied by the distance between the sections. For each animal, we took 10 equidistant semithin sections of the prosoma and of the ospisthosoma, for the tracheae, and another 10 semithin sections of each lung. The location of the first (starting) section was chosen at random within an interval of T, T_1 or T_2 (Fig. 1). As we used the same samples for evaluating both surface area and barrier thickness, we combined the Cavalieri principle with the vertical section method (Baddeley et al., 1986). The frontal plane of an animal was defined as the horizontal plane, while vertical planes were all planes perpendicular to the horizontal plane (Fig. 1). In each group, animals were rotated sequentially about the axis of the vertical planes, according to the systematic random sampling method (Gundersen and Jensen, 1987). We started at a randomly chosen angle within 0–18 ° from the original orientation (the transverse axis is 0 °) for the first animal and added 18 ° for each further animal (Fig. 1).

For the volume determinations from semithin sections, we used a light microscope with a drawing tube and a light box, on which we placed our test array (Perry et al., 1994). Tracheal volumes (wall and lumen) were evaluated by point-counting at a final magnification of 620× for the primary tracheae and of 1550× for the secondary tracheae. The secondary tracheae were divided into seven classes according to their inner diameters: class I, 1 μm and less; class II, between 1 and 2 μm; class III, between 2 and 3 μm; class IV, between 3 and 4 μm; class V, between 4 and 5 μm; class VI, between 5 and 6 μm; class VII, between 6 and 7 μm (Fig. 2). The total areas of the lung sections (tissue and lumen) were evaluated by point-counting at a final magnification of 620×.

The volumes of the wall and lumen of the secondary tracheae and of the lungs were determined from ultrathin sections by point-counting at a final magnification of 3260×, with the test grid placed directly onto transmission electron micrographs.

Surface areas and barrier thickness: vertical sections

The surface areas of the lungs were determined from semithin sections using 40 symmetrically distributed test fields per animal. The surface areas of the inner and outer surfaces and of the surfaces of the border between the cuticle and hypodermis were determined from their respective surface-area-to-volume ratios (S_V) multiplied by the volume of the lungs (tissue and lumen). The S_V of each component was determined by point- and intersection-counting sections at a final magnification of 1550× (Fig. 3A). The S_V was calculated as $S_V=2I/L$, where I is the number of intersections of the test lines with the surface and L is the total length of test lines covering the lung (tissue and lumen). Respiratory surface areas (S_R) were evaluated during measurements of barrier thickness (Fig. 3B) and are defined as those surfaces exposed to respiratory medium that are not connected by a

measuring line to another such surface. Points connected with measurement lines that left the field of measurement were not counted. The percentage of a surface area that is respiratory (%S_R) was calculated as $100I_R/(I_R+I_{NR})$, where I_R is the number of points falling on respiratory surfaces and I_{NR} is the number of points falling on non-respiratory surfaces.

Both the surface areas of the tracheae and barrier thickness were evaluated using transmission electron micrographs taken from ultrathin sections at the same positions as the semithin sections. The photographs were evaluated using a stereomicroscope with a drawing tube and a light box, on which we placed our test array (Perry et al., 1994). The data were pooled and evaluated for both groups of animals (Howard and Reed, 1998).

The areas of the inner and outer surfaces and of the surfaces of the border between the cuticle and hypodermis of all secondary tracheal classes were determined from their respective surface-area-to-volume ratios (S_V) multiplied by the volume of the respective tracheal class. The S_V of each tracheal class was determined by point- and intersection-counting of single tracheae at a final magnification of 3280× (classes I and II) or 1340× (classes III–VII). S_V and S_R were calculated as described for the lungs (Fig. 2F).

The barrier thickness of cuticular and hypodermal layers was measured in randomly chosen directions from transmission electron micrographs using the stereomicroscope and with a half-logarithmic ruler (Perry, 1981). The starting point of a measurement was selected in an unbiased way by the test array as the intersection of the test line with the surface (Figs 2F, 3B). The final magnification was 27 400× for class I tracheae, 13 600× for class II and III tracheae, 10 180× for tracheae of classes IV–VII and 13 900× for the lungs.

The harmonic mean lengths of the measured distances were calculated as:

$$l = N/\left(\sum_{i=1}^{N} l/l_i\right), \qquad (1)$$

where N is the number of measuring points and l is the harmonic mean length, calculated from the individual measured lengths l_i. The harmonic mean length was then converted to the harmonic mean barrier thickness as $\tau=\frac{2}{3}l$ (Weibel and Knight, 1964). According to Fick's first law, thin regions are more relevant for gas exchange than thick regions, so the harmonic mean, which weights in favour of small values, is more relevant than is the arithmetic mean. In the mathematical

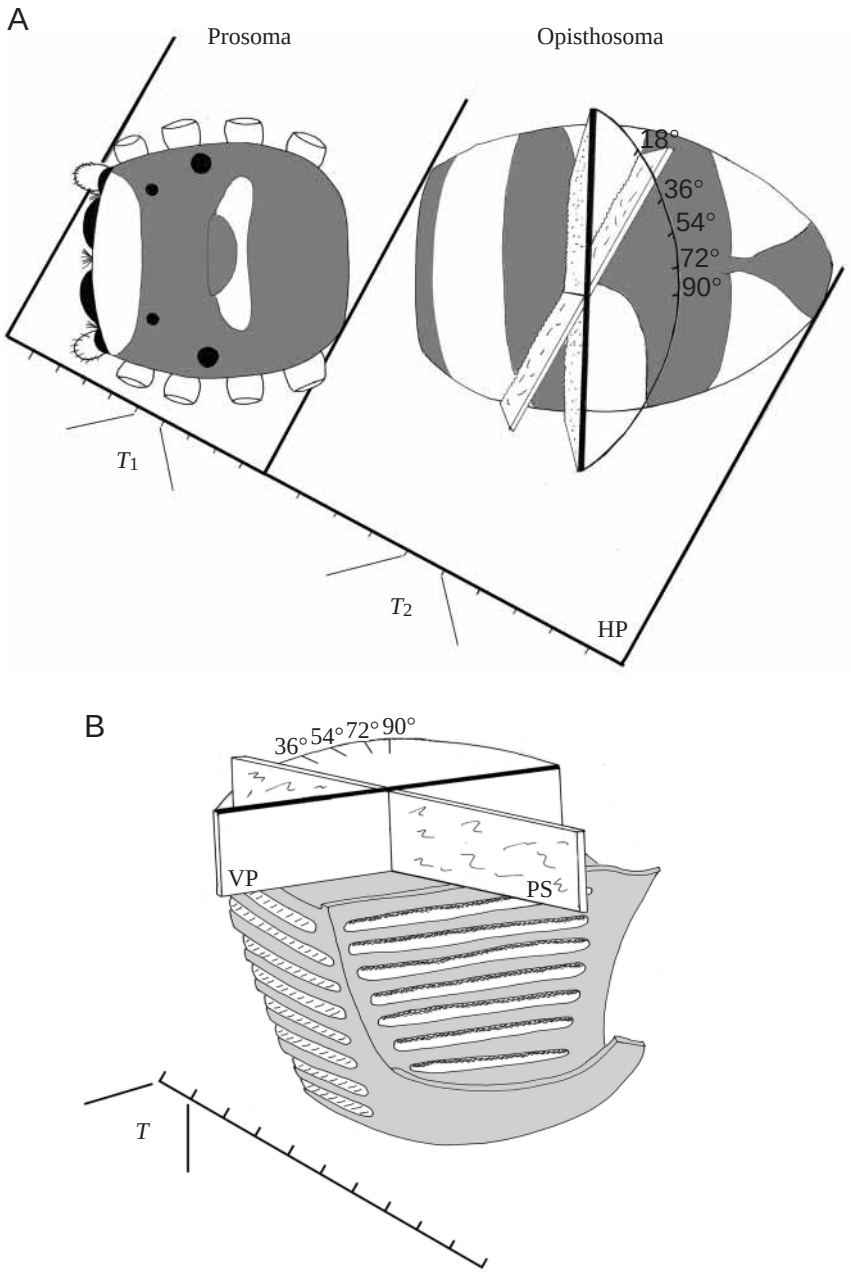

Fig. 1. (A) Schematic drawing of *Salticus scenicus* demonstrating the sampling methods for the combined Cavalieri principle and the vertical section method. The horizontal plane (HP) is the frontal plane of the animal. The pro- and opisthosoma were each cut into 10 pieces of equal length (sizes of sections indicated by T_1 and T_2). The plane of section was in the vertical axis. One example (20° from the transverse axis at 0°, marked by a heavy black line) is given. See text for further details. (B) Schematic drawing of a lung of *Salticus scenicus* demonstrating the sampling methods for the combined Cavalieri principle and the vertical section method. The horizontal plane is the frontal plane of the lung. The lung was cut into 10 pieces of equal length (T). The plane of section (PS) was in the vertical axis. One example (20° from the transverse axis at 0°, marked by a heavy black line) is given. VP, vertical plane.

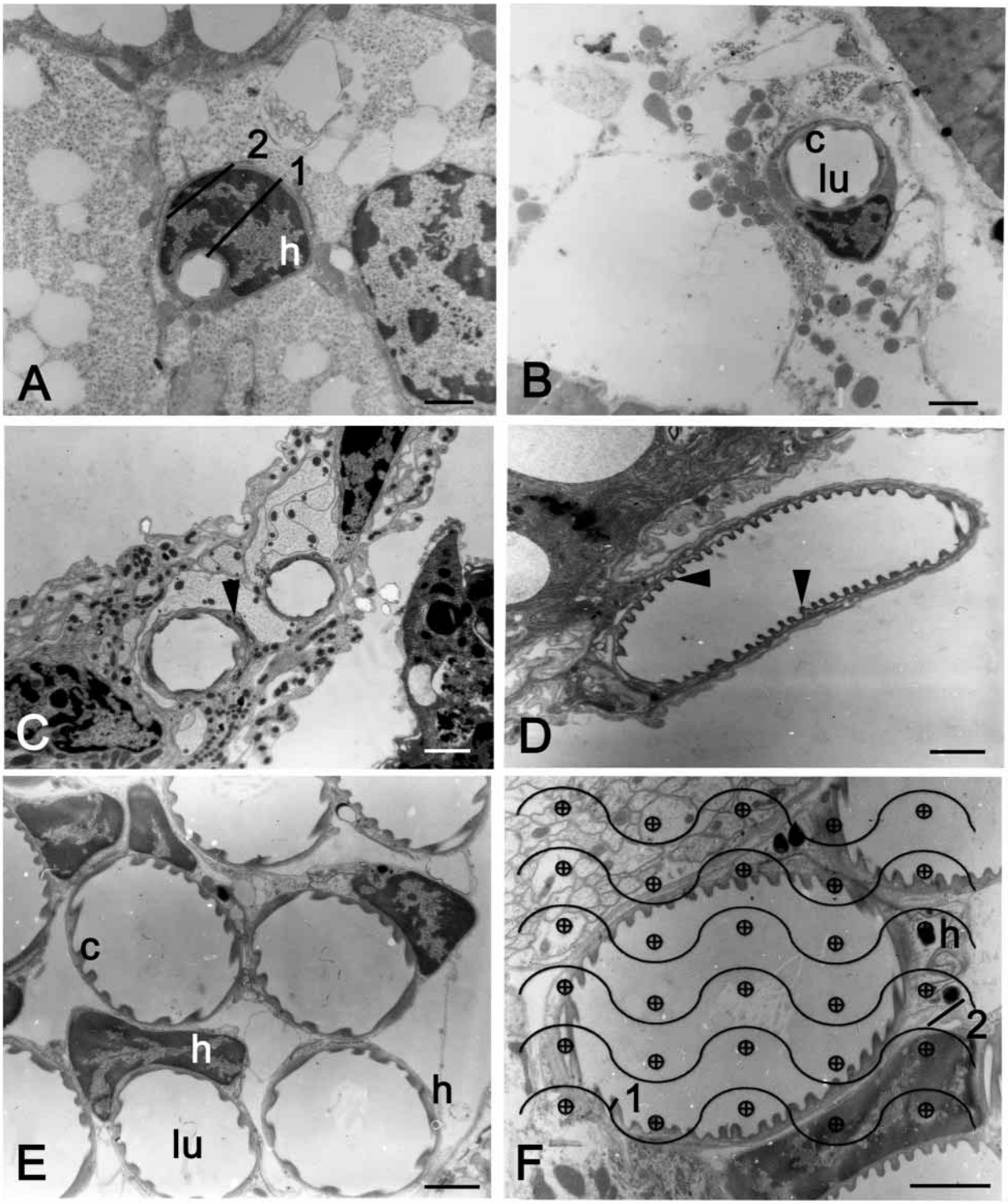

Fig. 2. Electron micrographs of tracheae of the different classes. (A) Class I trachea with a prominent hypodermis (h). Line 2 gives an example of a measurement line that connects two points at the outer surface, line 1 of a line that connects the inner with the outer surface of the trachea. (B) Class II trachea. c, cuticular lining; lu, lumen of the trachea. (C) Class III tracheae with a homogeneous hypodermis (arrowhead). (D) Class IV trachea. Note the prominent taenidia (arrowheads). (E) A bundle of class V tracheae, some showing a prominent hypodermis. (F) Class VI trachea overlaid with the test array used for the surface-to-volume ratio measurements and to select the starting points of the measurement lines for the barrier thickness. Line 1 gives an example of a measurement line that connects two points at the inner surface and line 2 of a line that connects two points at the outer surface. Scale bars in A and B represent 1 μm, those in C–F represent 2 μm.

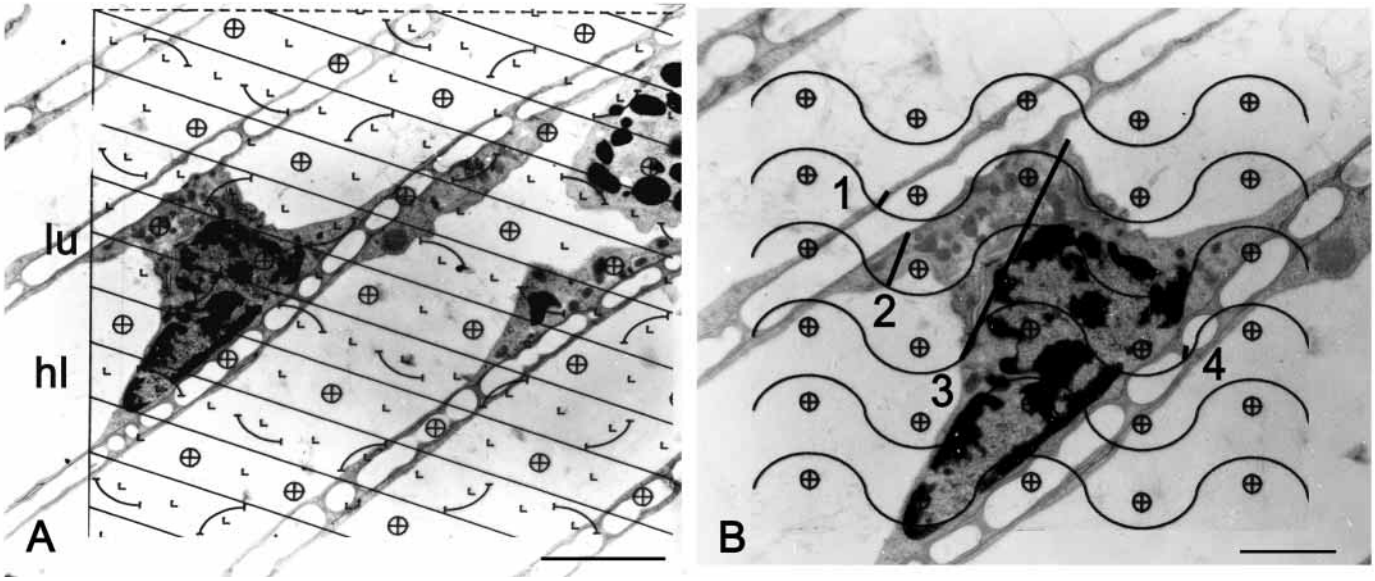

Fig. 3. (A) Determination of surface-to-volume ratios (S_V) with the test grid placed over a section of the lung. hl, haemolymph-filled lung space; lu, air-filled lung space. Scale bar, 5 μm. (B) Measurements of barrier thickness were made from electron micrographs; some measurement lines are given as an example. The starting points of measurements were chosen from the intersection of the test lines with the surface of the cuticular or hypodermal layers. Lines 1 and 2 are measurement lines that connect the inner surface (air-filled lung space) with the outer surface (haemolymph-filled lung space), line 3 is a measurement line that connects two points at the outer surface and line 4 is a measurement line that connects two points at the inner surface. Scale bar, 2 μm.

derivation for the determination from randomly oriented sections, the harmonic mean of measured lengths must be multiplied by the factor 2/3 to compensate for an overestimate due to the random orientation of the measured intercepts (Weibel and Knight, 1964).

Anatomical diffusion factor and diffusing capacity

The anatomical diffusion factors (ADFs) (Perry, 1978) were calculated as the surface areas with respect to body mass (as S/M_B) divided by the harmonic mean barrier thickness (τ) of the respective layers. For the inner surface (leading from the air to the haemolymph), we used the inner respiratory surface area for the ADF of the cuticle and the surface area of the border between the cuticle and hypodermis for the ADF of the hypodermis. For the outer surface (leading from the haemolymph to the air), we used the outer respiratory surface area for the ADF of the hypodermis and the surface area of the border between the cuticle and hypodermis for the ADF of the cuticle.

The morphological oxygen-diffusing capacities (from air to haemolymph) were calculated for each of the two layers as the product of the ADFs and Krogh's diffusion coefficient (K), corrected to 20 °C (Bartels, 1971; Krogh, 1919). For the hypodermis, we used the corrected published value for rat lung tissue (K=2.05×10^{-7} cm^2 min^{-1} kPa^{-1}) and for cuticle that for chitin (1.28×10^{-8} cm^2 min^{-1} kPa^{-1}). The total oxygen-diffusing capacity of the tracheal walls and lung epithelium (D_{O_2}) is calculated as the reciprocal of the sum of the reciprocal values of the diffusing capacities of cuticle (D_c) and hypodermis (D_h), respectively (Weibel, 1970/71):

$$1/D_{O_2} = 1/D_c + 1/D_h . \quad (2)$$

Statistical analyses

To evaluate the estimator variance, we calculated the standard deviation (S.D.) and coefficient of error (C.E.) of our barrier thickness measurements. Because τ is calculated from the harmonic mean of the intercept lengths and the S.D. for the harmonic mean is not defined, we calculated the S.D. and C.E. of the arithmetic mean of the intercept lengths. As S_V was evaluated on fields covering a single trachea, we calculated the estimator variance of S_V as the S.D. and C.E. of the values for each field.

For the Cavalieri principle, the precision of the estimate (total variance of the counted points or var$P$) depends on the noise (inaccuracy of the test array) and the variance of the sum of the areas (var$_{\Sigma area}$): var$P$=noise+var$_{\Sigma area}$ (Gundersen and Jensen, 1987; Howard and Reed, 1998). The noise indicates how much the estimate could change if the test array were placed differently. It is calculated as: $0.0724(b/\sqrt{a})\sqrt{n\Sigma P}$, where $(b/\sqrt{a})$ is the 'average profile shape', 30 for the tracheae and 4 for the lungs, n is the number of sections and ΣP is the sum of all counted points. The variance of the area is a function of the number of sections, and the calculation is based on a covariogram analysis of data from cross-sectional areas (Howard and Reed, 1998).

The coefficient of error is calculated from var$P$ and the sum of all counted points according to:

$$\text{C.E.}\,(\Sigma P) = \frac{\sqrt{\text{var}P}}{\Sigma P} \quad (3)$$

(Cruz-Orive, 1993; Howard and Reed, 1998).

To test the differences between the two groups of animals

Table 1. *Volumes of the tracheae and lungs for one animal from each test group*

Mean body mass, *N*=6 (mg)	Lung volume (cm^3)	C.E. (%)	Tracheal class	Prosoma volume (cm^3)	Opisthosoma volume (cm^3)	Entire body volume (cm^3)	C.E. (%)
Group A							
2.69	9.8×10^{-6}	0.3	I	2.51×10^{-8}	8.86×10^{-8}	11.37×10^{-8}	1.9
			II	15.10×10^{-8}	53.10×10^{-8}	68.20×10^{-8}	0.6
			III	2.51×10^{-8}	55.50×10^{-8}	58.01×10^{-8}	0.8
			IV		34.70×10^{-8}	34.70×10^{-8}	1.1
			V		28.80×10^{-8}	28.80×10^{-8}	1.8
			VI		5.30×10^{-8}	5.3×10^{-8}	4.7
			Total*	20.12×10^{-8}	186.26×10^{-8}	206.38×10^{-8}	
Group B							
5.28	14.0×10^{-6}	0.8	I	1.50×10^{-8}	15.60×10^{-8}	17.10×10^{-8}	2.1
			II	12.97×10^{-8}	91.70×10^{-8}	104.67×10^{-8}	0.8
			III	11.46×10^{-8}	109.95×10^{-8}	121.41×10^{-8}	0.9
			IV	11.99×10^{-8}	94.98×10^{-8}	106.97×10^{-8}	1.1
			V	1.73×10^{-8}	118.87×10^{-8}	120.60×10^{-8}	1.4
			VI		70.56×10^{-8}	70.56×10^{-8}	2.7
			VII		23.33×10^{-8}	23.33×10^{-8}	3.8
			Total	39.65×10^{-8}	524.99×10^{-8}	564.64×10^{-8}	

Secondary tracheae are divided into seven classes according to internal diameter, see Materials and methods.
C.E., coefficient of error.
*Total, the combined volumes of all secondary tracheae.
Values are means.

(volumes of respiratory organs, S_V, diffusion barrier and ADF) and between different classes of secondary tracheae (barrier thickness), we used *t*-test statistics.

Rates of oxygen consumption rates (respirometry)

The rates of O_2 consumption of female *Salticus scenicus* were measured using a Gilson differential respirometer. For these experiments, we used a different group of females (*N*=29) from those used for stereological measurements. All animals were fed with *Drosophila* spp. 3 days before the experiment. The rates of oxygen consumption were measured at 20 °C and 100 % relative humidity during the night and again during the following day at 25 °C and with an artificial light source, allowing a 2 h temperature equilibration time between these measurements. The measurement period extended over 12 h during darkness (one mean value) and 8 h in the light (observation periods of 1 h). Animals were placed in 15 ml flasks, 10 % KOH was placed in the centre well of the flasks to absorb CO_2 and the rate of O_2 consumption was converted to volume of O_2 utilised per unit time per gram tissue ($\mu l\,min^{-1}\,g^{-1}$) at STPD.

Results

Volumetry

The primary tracheae possess a thick hypodermis and also a thick cuticular lining with prominent trichomes. Some test measurements of the barrier thickness resulted in values approximately 10 times greater than for secondary tracheae. Primary tracheae will, therefore, show a very low lateral diffusing capacity in comparison with secondary tracheae, so only the volumes of primary tracheae were determined. In small animals (group A), the mean volume of the primary tracheae was $107\times10^{-8}\,cm^3$ (0.10 % of the total body volume without legs); in large animals (group B) it was $208\times10^{-8}\,cm^3$ (0.09 % of body volume).

The dimensions of the secondary tracheae differ in the two groups of animals tested. In group A, the diameters of the secondary tracheae range from 1 to 6 μm; in group B, tracheae with diameters of 7 μm are also present. In the prosoma, tracheae with diameters of 1–3 μm occur in group A animals, while tracheae with diameters of 1–5 μm are found in group B animals.

The volume of all secondary tracheae was $206\times10^{-8}\,cm^3$ for group A (0.18 % of body volume) and $565\times10^{-8}\,cm^3$ for group B (0.23 % of body volume). This results in a total tracheal volume of $313\times10^{-8}\,cm^3$ for group A (0.28 % of body volume) and $773\times10^{-8}\,cm^3$ for group B (0.32 % of body volume). The absolute volumes of the seven tracheal classes, given separately for the pro- and opisthosoma, are shown in Table 1 and are given as a percentage of the volume of all secondary tracheae (entire body) in Fig. 4. In both groups, the opisthosoma makes up the major part of the tracheal volume. The volume of all secondary tracheae/M_B was $76.6\times10^{-8}\,cm^3\,mg^{-1}$ in group A and $107\times10^{-8}\,cm^3\,mg^{-1}$ in group B and differed significantly between the groups ($P<0.01$). In group A, tracheae of class II make up the greatest percentage of the volume, followed by classes III and IV. In

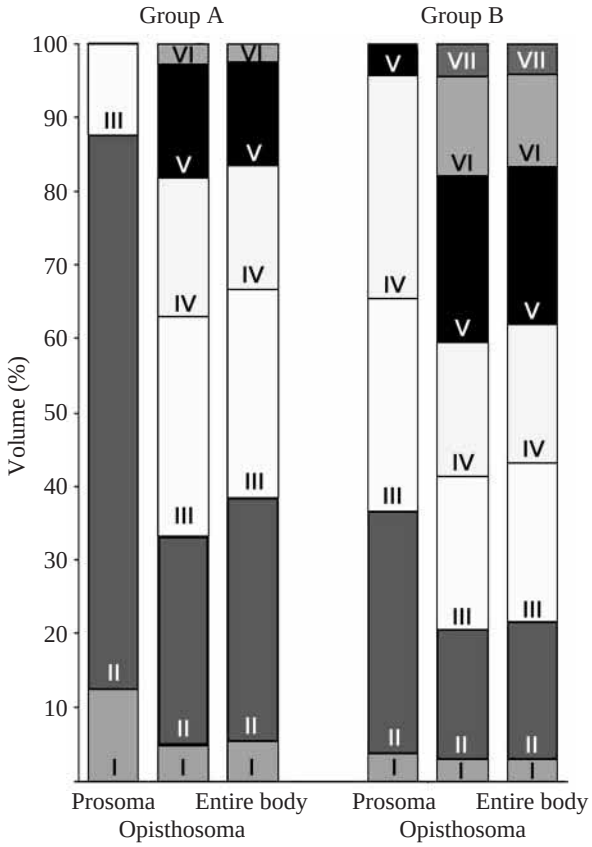

Fig. 4. Volumes of the tracheal classes (I–VII) as a percentage of the volume of the prosoma, the opisthosoma and the entire body for the two groups of animals.

group B, tracheal classes II–V make up most of the volume. The relative contributions of the volumes of the lumen and of the cuticular and hypodermal layers to the total volume of the tracheal classes are shown in Fig. 5. The proportion occupied by cuticle is very similar in all tracheal classes, while the proportion occupied by the lumen increases and that occupied by the hypodermal layer decreases as the diameter of the tracheal class increases.

The mean values for lung volume were $9.8\times10^{-6}\pm0.58\times10^{-6}$ cm^3 (N=6, mean ± S.D., range 8.9×10^{-6} to 10.7×10^{-6} cm^3) for group A animals and $14\times10^{-6}\pm0.86\times10^{-6}$ cm^3 (N=6, mean ± S.D., range 12.8×10^{-6} to 15.4×10^{-6} cm^3) for group B animals (Table 1). This gives a lung volume/M_B ratio of 3.64×10^{-6} $cm^3\,mg^{-1}$ for group A animals and 2.65×10^{-6} $cm^3\,mg^{-1}$ for group B animals. These values differ significantly between the two groups (P<0.0001). Fig. 6 shows a comparison between the volumes of air-filled lumen, haemolymph-filled lumen, cuticular layer and hypodermal layer of the two groups. The proportion of the lung space filled with haemolymph is more than 50 % of the total lung volume in both groups, while the air-filled lumen makes up 24 % of the volume in group A animals and 22 % in group B animals. The cuticular and hypodermal layers share the rest of the total lung volume and make up similar proportions in both groups.

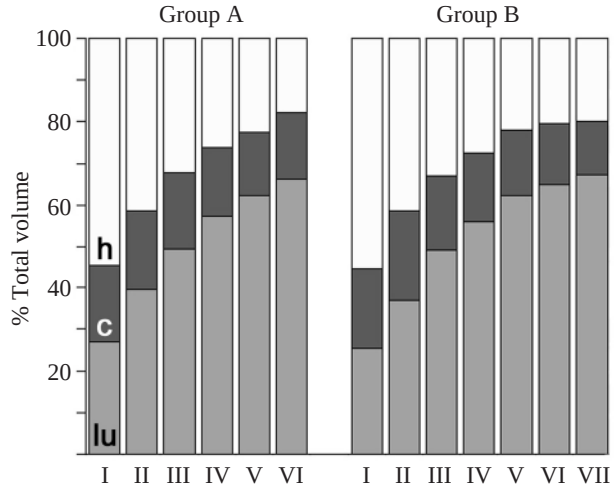

Fig. 5. Volumes of the lumen (lu) and the cuticular (c) and hypodermal (h) layers of the tracheal classes as a percentage of the total volume of each secondary tracheal class in group A and group B spiders.

Surface-area-to-volume ratios, surface areas and anatomical diffusing factors

Surface-area-to-volume ratios (S_V) are shown in Table 2 for the tracheae and lungs. S_V values are greatest for the smallest tracheae and decrease with increasing tracheal diameter, for both the cuticle and hypodermis. The S_V for the inner surface and for the surface between the cuticle and hypodermis of the lungs is significantly different between group A and group B (P<0.01), but there are no significant differences in any tracheal class between the two animal groups. The S_V of the outer surface area is significantly different between group A and group B for all tracheal classes (P<0.001), but not for the lungs.

Total surface areas, respiratory surface areas and respiratory surface areas/M_B are given in Table 3. The surface area

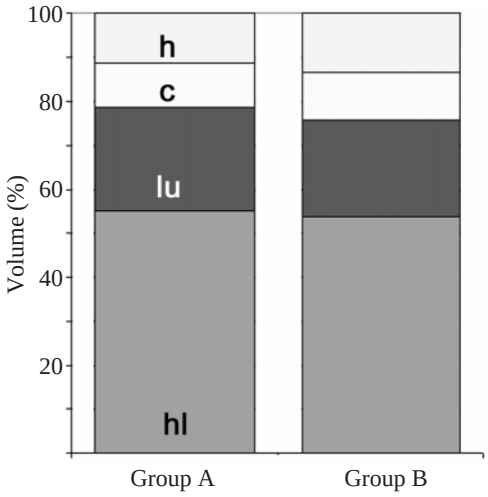

Fig. 6. Volumes of the haemolymph-filled lung space (hl), the air-filled lung space (lu) and the cuticular (c) and hypodermal (h) layers as a percentage of the total lung volume.

Table 2. *Statistical results for measured line lengths and surface-area-to-volume ratios*

	Tracheal classes and lungs	Arithmetic mean group A/group B (μm)	S.D. group A/group B	C.E. group A/group B (%)	Number of measurements group A/group B
Line length, l_i					
Cuticle	I	0.18/0.19	0.10/0.12	2.3/2.5	601/596
	II	0.27/0.27	0.14/0.17	2.5/2.7	436/552
	III	0.28/0.27	0.16/0.18	2.5/3.0	529/472
	IV	0.25/0.29	0.16/0.20	2.3/2.5	745/729
	V	0.31/0.34	0.20/0.21	2.4/2.6	726/591
	VI	0.35/0.31	0.22/0.18	2.9/2.7	463/464
	VII	0.38	0.22	2.8	426
	Lungs	0.17/0.19	0.15/0.16	2.9/2.6	936/993
Hypodermis	I	0.25/0.27	0.31/0.34	4.9/4.9	601/596
	II	0.33/0.48	0.33/0.56	4.7/5.0	436/552
	III	0.50/0.30	0.56/0.31	4.9/4.8	529/472
	IV	0.35/0.34	0.48/0.45	4.9/4.8	745/729
	V	0.35/0.33	0.48/0.40	4.9/4.9	726/591
	VI	0.43/0.28	0.46/0.24	4.9/4.0	463/464
	VII	0.34	0.31	4.4	426
	Lungs	0.34/0.36	0.47/0.50	4.8/4.5	936/993

S_V	Tracheal class and lungs	Mean group A/group B (cm^{-1})	S.D. group A/group B	C.E. group A/group B (%)	Number of fields evaluated group A/group B
Inner surface	I	16020/16476	8335/7209	5.0/3.6	110/92
	II	12681/14642	5069/5642	3.9/3.6	104/112
	III	10573/9403	3544/3965	3.4/4.1	100/104
	IV	8812/7688	3098/2546	3.6/3.3	95/103
	V	7127/7483	1890/2385	2.9/3.4	86/86
	VI	6225/6577	1399/1596	3.7/3.1	38/62
	VII	6081	1467	3.1	60
	Lungs	3548/3929	1088/1653	2.1/2.9	221/217
Surface between cuticle and hypodermis					
	I	12137/11988	5041/4871	3.9/4.2	110/92
	II	8742/9468	2991/3942	3.4/3.9	104/112
	III	7360/6400	1993/1483	2.7/2.3	100/104
	IV	6398/5422	1497/887	2.4/1.6	95/103
	V	4861/4635	917/851	2.0/1.9	86/86
	VI	4150/4635	771/703	3.0/2.3	38/62
	VII	3515	684	2.5	60
	Lungs	3087/3514	988/1056	2.2/2.0	221/217
Outer surface	I	21408/20506	8055/8037	4.6/4.1	110/92
	II	14090/15273	4435/5500	3.1/3.4	104/112
	III	11781/10109	3763/2701	3.1/2.6	100/104
	IV	9039/7756	2648/1929	3.0/2.5	95/103
	V	7119/6153	1534/1381	2.3/2.4	86/86
	VI	6064/5375	983/894	2.6/3.1	38/62
	VII	4640	812	2.3	60
	Lungs	3702/3964	1080/1654	2.0/2.3	221/217

S_V, surface-area-to-volume ratio; C.E., coefficient of error.

between cuticle and hypodermis is identical with the respiratory surface area, while the inner and outer respiratory surface areas are smaller than the total inner and outer surface areas. In all tracheae and also in the lungs, the inner respiratory surface area is greater than the outer one. This is because of the heterogeneity of the hypodermis and the enlargement of the surface area due to the taenidia (Figs 2, 3).

For the ADF (Table 4) of all secondary tracheae, there is a

Table 3. *A comparison of the surface areas of tracheae and lungs for one animal from group A and one from group B*

Mean body mass, *N*=6 (mg)	Tracheal class and lungs	Inner surface area (cm^2)	Inner respiratory surface area (cm^2)	Inner respiratory surface area/ body mass ($cm^2\,g^{-1}$)	Surface area between cuticle and hypodermis (cm^2)	Outer surface area (cm^2)	Outer respiratory surface area (cm^2)	Outer respiratory surface area/ body mass ($cm^2\,g^{-1}$)
Group A								
2.69	I	1.8×10^{-3}	1.53×10^{-3}	0.57	1.38×10^{-3}	2.40×10^{-3}	1.23×10^{-3}	0.46
	II	8.77×10^{-3}	7.09×10^{-3}	2.64	5.95×10^{-3}	9.60×10^{-3}	4.81×10^{-3}	1.79
	III	6.13×10^{-3}	4.57×10^{-3}	1.70	4.27×10^{-3}	6.80×10^{-3}	3.96×10^{-3}	1.47
	IV	3.05×10^{-3}	2.45×10^{-3}	0.91	2.22×10^{-3}	3.10×10^{-3}	1.98×10^{-3}	0.73
	V	2.05×10^{-3}	1.52×10^{-3}	0.56	1.40×10^{-3}	2.05×10^{-3}	1.29×10^{-3}	0.48
	VI	0.30×10^{-3}	0.23×10^{-3}	0.08	0.22×10^{-3}	0.30×10^{-3}	0.21×10^{-3}	0.07
	Total	22.10×10^{-3}	17.38×10^{-3}	6.46	15.44×10^{-3}	24.21×10^{-3}	13.46×10^{-3}	5.01
	Lungs	34.9×10^{-3}	29.5×10^{-3}	10.85	30.2×10^{-3}	33.5×10^{-3}	30.8×10^{-3}	11.30
Group B								
5.28	I	2.80×10^{-3}	2.35×10^{-3}	0.45	2.05×10^{-3}	3.50×10^{-3}	1.75×10^{-3}	0.33
	II	15.30×10^{-3}	11.60×10^{-3}	2.20	9.91×10^{-3}	15.90×10^{-3}	8.22×10^{-3}	1.56
	III	11.40×10^{-3}	8.24×10^{-3}	1.56	7.77×10^{-3}	12.30×10^{-3}	7.29×10^{-3}	1.38
	IV	8.20×10^{-3}	6.17×10^{-3}	1.17	5.80×10^{-3}	8.30×10^{-3}	5.42×10^{-3}	1.03
	V	9.00×10^{-3}	6.47×10^{-3}	1.22	5.59×10^{-3}	7.40×10^{-3}	4.70×10^{-3}	0.89
	VI	4.60×10^{-3}	2.79×10^{-3}	0.53	2.74×10^{-3}	3.80×10^{-3}	2.68×10^{-3}	0.51
	VII	1.40×10^{-3}	0.92×10^{-3}	0.17	0.82×10^{-3}	1.10×10^{-3}	0.72×10^{-3}	0.14
	Total	52.70×10^{-3}	38.55×10^{-3}	7.30	34.68×10^{-3}	52.30×10^{-3}	30.77×10^{-3}	5.83
	Lungs	54.50×10^{-3}	47.70×10^{-3}	8.87	49.2×10^{-3}	54.00×10^{-3}	50.70×10^{-3}	9.43

Table 4. *Anatomical diffusing factors per body mass for inner and outer respiratory surface areas*

		Anatomical diffusing factor	
Mean body mass, *N*=6 (mg)	Tracheal class and lungs	Inner surface cuticle/hypodermis ($cm\,g^{-1}$)	Outer surface cuticle/hypodermis ($cm\,g^{-1}$)
Group A			
2.69	I	$61.40\times10^3/64.37\times10^3$	$55.40\times10^3/57.17\times10^3$
	II	$192.46\times10^3/189.54\times10^3$	$161.60\times10^3/153.08\times10^3$
	III	$121.40\times10^3/108.57\times10^3$	$113.55\times10^3/100.80\times10^3$
	IV	$71.72\times10^3/73.29\times10^3$	$65.10\times10^3/65.25\times10^3$
	V	$38.79\times10^3/45.54\times10^3$	$35.70\times10^3/41.88\times10^3$
	VI	$5.05\times10^3/5.56\times10^3$	$4.83\times10^3/5.18\times10^3$
	Total	$490.83\times10^3/486.87\times10^3$	$436.18\times10^3/423.36\times10^3$
	Lungs	$1367\times10^3/1324\times10^3$	$1413\times10^3/1334\times10^3$
Group B			
5.28	I	$49.03\times10^3/44.70\times10^3$	$42.70\times10^3/38.17\times10^3$
	II	$162.06\times10^3/129.40\times10^3$	$138.40\times10^3/107.41\times10^3$
	III	$124.73\times10^3/140.29\times10^3$	$117.50\times10^3/131.58\times10^3$
	IV	$85.91\times10^3/90.56\times10^3$	$80.80\times10^3/84.61\times10^3$
	V	$81.78\times10^3/93.90\times10^3$	$74.50\times10^3/74.73\times10^3$
	VI	$36.58\times10^3/41.80\times10^3$	$35.84\times10^3/40.97\times10^3$
	VII	$10.60\times10^3/11.30\times10^3$	$9.45\times10^3/9.89\times10^3$
	Total	$550.74\times10^3/551.95\times10^3$	$499.19\times10^3/487.37\times10^3$
	Lungs	$997\times10^3/961\times10^3$	$1046\times10^3/973\times10^3$

significant difference in the hypodermis and the cuticle between groups A and B ($P<0.01$). In the lungs, the ADF for both the cuticle and the hypodermis also show significant differences between groups A and B ($P<0.001$ for cuticle and $P<0.01$ for hypodermis). Respiratory surface areas and ADFs are greatest for class II tracheae in both groups of animals followed by class III for group A and classes III–V for group B, while in both groups classes VI and VII show the smallest ADFs.

Table 5. *Diffusing capacities for oxygen of the tracheae and lungs*

Tracheal class and lungs	Diffusing capacity ($\mu l\,min^{-1}\,g^{-1}\,kPa^{-1}$) Group A, M_B 2.69 mg	Group B, M_B 5.28 mg
I	0.74	0.59
II	2.32	1.93
III	1.45	1.51
IV	0.87	1.04
V	0.47	0.99
VI	0.06	0.44
VII		0.13
Total	5.91	6.63
Lungs	16.4	12.0

*M_B, mean body mass.

Barrier thickness

Fig. 7 shows that the barrier thickness is smaller for the class I tracheae for both cuticle and hypodermis, resulting in a diffusion barrier of 0.17 μm for group A and 0.18 μm for group B animals. Barrier thickness did not differ significantly between groups A and B when considering the single tracheal classes. Looking at groups A and B separately, the diffusion barrier of class I tracheae is significantly thinner than that of all the other classes (P<0.0001) for both the cuticular and the hypodermal layers. The diffusion barriers for the walls of class II–VII tracheae within each group are very similar (0.24–0.32 μm in group A and 0.24–0.30 μm in group B). The slight differences observed are due mainly to differences in the thickness of the hypodermal layer. The barrier thickness of the lungs is less than 0.1 μm for both cuticular and hypodermal layers in the two groups of animals, and this gives a total diffusion barrier of 0.164 μm for group A and 0.186 μm for group B. There is no significant difference in the barrier thickness of the lungs between group A and group B animals. Statistical results for barrier thickness measurements are given in Table 2.

Diffusing capacities

In both groups of animals, more than half the lateral diffusing capacity of the tracheae for oxygen (D_{O_2}) resides in class II and class III tracheae, followed by classes IV, V and I (Table 5). The largest tracheae (VI and VII) make up the smallest proportion of the total D_{O_2}.

The volume-to-body-mass ratio of the tracheae and lungs and the ADF for the hypodermis and cuticle in the tracheae and lungs showed significant differences between groups A and B. Thus, the diffusing capacities for oxygen are also significantly different between the two groups for both secondary tracheae and lungs.

A calculation of the whole oxygen-diffusing capacity of respiratory organs from the D_{O_2} of the lungs and that of the secondary tracheae shows that the tracheae make up 26.5 % of the total D_{O_2} in group A animals and 36 % in group B animals. No value for K_{CO_2} is available in the literature, so we can only estimate that the diffusing capacity for carbon dioxide (D_{CO_2}) is approximately 30 times greater than D_{O_2}.

Rates of oxygen consumption

The rates of oxygen consumption $\dot{V}_{O_2}$ of 29 animals during light conditions (M_B=4.49±2.3 mg, mean ± S.D., range 1.8–9.1 mg, N=29) were measured every hour. The mean values for each animal for the entire time of measurement was 16.1±4.2 $\mu l\,min^{-1}\,g^{-1}$ (mean ± S.D., range 9.4–25.8 $\mu l\,min^{-1}\,g^{-1}$; N=29) at STPD. During darkness, a single $\dot{V}_{O_2}$ measurement was taken at the end of the 12 h period for 24 animals (M_B=4.34±2.1 mg, mean ± S.D., range 1.8–9.1 mg; N=24). The $\dot{V}_{O_2}$ was 4.9±1.0 $\mu l\,min^{-1}\,g^{-1}$ (mean ± S.D., range 3.1–6.6 $\mu l\,min^{-1}\,g^{-1}$; N=24) at STPD.

Taking 3.6 $\mu l\,min^{-1}\,g^{-1}$, which is the rate of oxygen consumption of a resting spider at 25 °C, a Q_{10} of 1.35 can be calculated by taking the value for the same animal at 20 °C (3.1 $\mu l\,min^{-1}\,g^{-1}$). Using this Q_{10} value to correct the resting rates gives a mean resting $\dot{V}_{O_2}$ of 5.2 $\mu l\,min^{-1}\,g^{-1}$ at 25 °C.

Using similar calculations, a typical group A spider raised its metabolic rate during the day to approximately 3.3 times that at night and a typical group B spider raised its metabolic rate by 3.1-fold.

Discussion

Methods

The tracheal and lung tissue was well conserved by the fixation procedure so that no distortion influenced the measuring processes. As a result of using vertical sections, the variance among animals will differ systematically according to the plane of sectioning. For this reason, it was necessary to pool

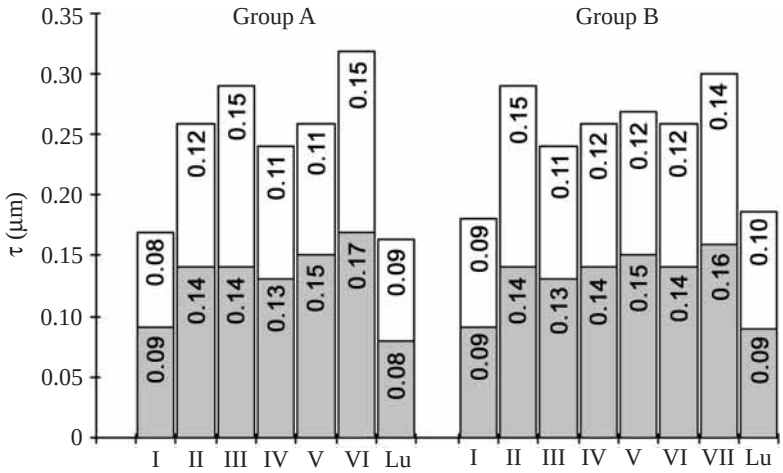

Fig. 7. Barrier thickness (τ) of the cuticle (shaded area of the columns) and the hypodermis (unshaded area of the columns) for tracheal classes I–VII and for the lungs (Lu).

samples, so we could not determine the between-animal variance. This is generally assumed to be approximately 15 % of the mean (L. M. Cruz-Orive, personal communication). The coefficient of error (C.E.) of all measured values is less than 5 % (Tables 1, 2), so the observed variation in volumes, surface areas, barrier thickness and ADF is dominated by the biological variation.

The calculated diffusing capacities are only estimates and could be erroneous because we used Krogh's diffusion constant (*K*) for chitin measured for the 54 µm thick intersegmental membranes of *Oryctes* spp. larvae (Krogh, 1919). Although *K* is normalised to unit thickness, the chitin used to determine this *K* value was quite thick by respiratory standards. The constant may, therefore, be too low for the lungs and tracheae of jumping spiders, and the diffusing capacities could be even greater than reported here.

Rates of oxygen consumption were measured during dark periods at 20 °C, i.e. under conditions that are considered to give resting rates in jumping spiders (Anderson and Prestwich, 1982; Anderson, 1996). In the light, the temperature was elevated to 25 °C, which corresponds to daytime temperatures under natural conditions.

Comparison of ADFs and diffusion barriers

Differences in ADF between the tracheal classes are largely dependent on the volumes and surface areas; the small differences in barrier thickness are of minor importance. As the cuticular layer of the tracheal wall is slightly thicker than that of the hypodermal layer in all tracheal classes and as Krogh's diffusion constant for chitin is lower than that for the hypodermal layer, the cuticular lining is the limiting factor for the diffusion barrier.

Comparison of diffusing capacities

The proportionally low volume of the secondary tracheae in the prosoma (Table 1) means that the diffusing capacity of the tracheal system in this part of the body is also low compared with that in the opisthosoma (less than 10 % of opisthosoma values in both groups of animals).

In the group B animals, the D_{O_2} of all secondary tracheae is significantly greater than in the smaller animals of group A, while the D_{O_2} of the lungs is significantly smaller. Interestingly, the distributions of the total diffusing capacity of the lungs and tracheae in large and small *Salticus scenicus* is different: large animals have proportionally more diffusing capacity in the tracheae (36 %) than do small ones (27 %). It is possible that this observed difference in diffusing capacity could be explained as an adaptation to meet the greater local oxygen demands of the maturing gonads in the opisthosoma of the more mature animals in group B.

Comparison with insect tracheal systems

The tracheal system of insects differs from that of jumping spiders in having a much wider range of diameters. The secondary tracheae of *S. scenicus* have diameters that can best be compared with tracheae just before the final terminations (tracheoles) in insects. In insects, barrier thickness is lowest in tracheoles and increases with increasing tracheal diameter (Schmitz and Perry, 1999). In jumping spiders, the walls of all secondary tracheae have a similar barrier thickness, but it tends to be reduced in the smallest tracheae. In the stick insect *Carausius morosus*, tracheoles with diameters of up to 1 µm have a total barrier thickness of 0.15 µm (cuticular layer 0.03 µm, hypodermal layer 0.12 µm); in tracheae with diameters of 2–5 µm, this is increased to 0.28 µm (cuticular layer 0.07 µm, hypodermal layer 0.21 µm) (Schmitz and Perry, 1999). Thus, the total barrier thickness of the tracheal walls of *C. morosus* is similar to that in *S. scenicus*, but the cuticular layer, which has a very low Krogh's constant, is 2–3 times thinner.

In *C. morosus*, approximately three-quarters of the lateral diffusing capacity lies in the tracheoles. In more active insects, this proportion is presumed to be even greater. In jumping spiders, the tracheal system is not homogeneously distributed, as it is in insects, but is mainly situated in the opisthosoma. The majority of the diffusing capacity lies in tracheae with diameters of 2–3 µm and not in the narrowest ones. In comparison, the diffusing capacity of the rest of the tracheal system is restricted mainly by the volumes and not by the diffusion barrier. As a result, the lateral diffusing capacity of the entire tracheal system of a 4.6 mg *C. morosus* instar is approximately 10 times greater than that of a *S. scenicus* of similar body mass.

The primary tracheae in *S. scenicus* appear to be structurally comparable with the air sacs of insects, which are presumed to have a very minor gas-exchange function. Thus, primary tracheae of jumping spiders could function in gas storage when the spiracle is closed, in a manner similar to the air sacs in insects, but without being ventilated.

Comparison of the lungs of Salticus scenicus *with the lungs of* Tegenaria *spp.*

Our data can best be compared with measurements made in *Tegenaria* spp. (Agelenidae) (Strazny and Perry, 1984). The S_V of the lungs measured in two animals with body mass of 27 and 28 mg was between 2100 and 2500 cm^{-1}, which is clearly less than in *S. scenicus* (3550–3900 cm^{-1}). The resulting value for inner lung surface per unit body mass (S_L/M_B) was 9–12.7 $cm^2\,g^{-1}$, which is in the same range as in *S. scenicus* (8.9–10.9 $cm^2\,g^{-1}$). The diffusion barrier was at least twice as thick in *Tegenaria* spp. as in *S. scenicus*. The resulting D_{O_2} was 4.3–9.2 $\mu l\,min^{-1}\,g^{-1}\,kPa^{-1}$, which is clearly less than in *S. scenicus* (12–16.4 $\mu l\,min^{-1}\,g^{-1}\,kPa^{-1}$). Thus, compared with these *Tegenaria* spp., the lungs of *S. scenicus* are morphologically optimised for gas exchange by a reduction in the thickness of the diffusion barrier rather than by an enlargement of the surface area.

Comparison of rates of O_2 consumption

Data on the rates of O_2 consumption of jumping spiders with a similar body mass to that of *S. scenicus* are restricted to a small number of species. Measurements were all carried out

Table 6. *Required ΔP_{O_2} of the lungs and tracheae of* Salticus scenicus *resulting from a comparison of* D_{O_2} *and* $\dot{V}_{O_2}$ *per body mass during rest, mean activity and estimated peak metabolic activity in the two groups of animals*

		ΔP_{O_2} (kPa)	
Respiratory organ		Group A, M_B 2.69 mg	Group B, M_B 5.28 mg
Lungs	Rest	0.30	0.40
	Mean activity	0.98	1.34
	Maximum	2.20	3.00
Secondary tracheae	Rest	0.83	0.7
	Mean activity	2.70	2.40
	Maximum	6.10	5.40
Lungs and secondary tracheae	Rest	0.22	0.26
	Mean activity	0.72	0.86
	Maximum	1.06	1.93

M_B, mean body mass; D_{O_2}, oxygen-diffusing capacity; $\dot{V}_{O_2}$, rate of oxygen uptake; ΔP_{O_2}, partial pressure of oxygen difference.

during the hours of darkness at 20 °C. *Metaphidippus vitis* (M_B=5.7 mg) has a $\dot{V}_{O_2}$ of 6.67 µl min^{-1} g^{-1} (Greenstone and Bennett, 1980), *Sarinda hentzi* (M_B=4.6 mg) has a $\dot{V}_{O_2}$ of 7.23 µl min^{-1} g^{-1} (Anderson, 1996) and *Zygoballus rufipes* (M_B=3 mg) has a $\dot{V}_{O_2}$ of 3.3 µl min^{-1} g^{-1} (Anderson, 1996). These values are in the same range as those measured here for *S. scenicus*. The mean values for $\dot{V}_{O_2}$ of *S. scenicus* during the day were approximately three times the resting rates. The maximum measured $\dot{V}_{O_2}$ was approximately nine times the mean resting rate, and there was a 12.9-fold increase from resting to activity when looking at the extreme values during the day. However, since this comparison is made between oxygen consumption rates of different animals, it might be due to individual variation, with some animals showing extreme rates for their size. One can estimate a reasonable peak $\dot{V}_{O_2}$ of 30–40 µl min^{-1} g^{-1} by taking the lowest resting values and multiply by 10. Although the maximal rate of oxygen consumption of spiders in general lies between 2 and 10 times the resting rate (Prestwich, 1983; Anderson and Prestwich, 1985), the aerobic scope of jumping spiders is greater than for species with less-developed tracheal systems. In addition, the rate of oxygen consumption increases during activity, not only during recovery from activity (Prestwich, 1983).

How do the tracheae of Salticus scenicus *function?*

Between 90 and 96 % of the diffusing capacity of the tracheal system in both size groups of *Salticus scenicus* resides in the opisthosoma. All classes of secondary tracheae that end in the haemolymph have close contact with the organs, e.g. gonads and fat body, but only penetrate into the gut and the nervous system (Schmitz and Perry, 2000). The remainder of the diffusing capacity of the tracheal system lies in the prosoma. A bundle of secondary tracheae (diameters 1–5 µm) runs parallel to the gut, passes the petiolus and enters the prosoma, where the tracheae end in or near the central nervous system and, to a lesser degree, in the gut epithelium (Schmitz and Perry, 2000). Since the large animals were sexually mature females whereas the smaller ones were not mature, we conclude that the relatively large proportion of tracheae present in the opisthosoma of large animals selectively serves the metabolically active, maturing gonads. As a secondary function, the tracheae in the prosoma are in direct contact with the nervous system and the gut epithelium, and they are, therefore, less effective in oxygenating the muscles, which they do not penetrate. For these reasons, the hypothesis that tracheae are necessary to provide oxygen to the leg muscles during phases of intense activity (e.g. escape or struggling) when fluid exchange between the opisthosoma and prosoma is interrupted (Anderson and Prestwich, 1975) can be rejected. This correlates with the observation that in *S. scenicus*, which is an ambush predator that actively patrols its territory, activity is dominated by walking, short sprints or occasional escape behaviour. Continuous intensive locomotion, which would need long-lasting pressure isolation between the pro- and opisthosoma, is not part of the normal behavioural pattern.

It is possible, however, that, even if the proportion of the tracheae in the prosoma were quite small, their role in the nervous system could be quite large. A small part of the total diffusing capacity of the tracheal system can meet the entire needs of the nervous system. Jumping spiders possess very well-developed eyes that are used for orientation, so the processing of information coming from the eyes is very important. In this context, is interesting to note that, although the stigma for the tracheae lies in the posterior opisthosoma, the tracheae are bundled as they pass the lungs and enter the petiolus, thus reducing their lateral diffusing capacity at this point and enhancing their function in diffusional gas transport.

In contrast to the jumping spiders, tracheae in the Uloboridae enter the legs. Measurements of the cross-sectional areas of tracheae in the legs have shown that the tracheae are best developed in those species that show active web-monitoring behaviour. These animals will, therefore, have a greater oxygen demand in their legs, and the main function of the tracheae in this system seems to be the transport of oxygen to the prosoma and legs (Opell, 1987, 1990, 1998).

From our results, we propose the following model for the functional morphology of the tracheal system in *Salticus scenicus*: the primary tracheae act as gas storage sites in a similar way to the air sacs of insects and thus act as a buffer during periods when the spiracle is closed. The similarity in the thickness of the walls of all classes of secondary tracheae is consistent with the hypothesis that they function as ‘tracheal lungs’ and that lateral diffusion to the haemolymph indirectly supplies some organs with oxygen. This is of special interest if one considers that haemocyanin is present as a respiratory pigment in the haemolymph. Secondary tracheae could also be very efficient in CO_2 release if the whole surface serves for CO_2 exchange. Thus, CO_2 stored in the tissues or haemolymph could be removed very quickly *via* the tracheal system.

Secondary tracheae thus combine two functions: (i) transport of oxygen to the prosoma supplying mainly the nervous system and the gut and (ii) oxygenation of the haemolymph by acting as 'tracheal lungs'. The transport function is particularly important in the tracheae that run as bundles from the spiracle to the prosoma (Schmitz and Perry, 2000). The function as 'tracheal lungs' is especially relevant for tracheae with diameters of 2–3 μm since these possess the greatest diffusing capacity.

How does the double respiratory system of Salticus scenicus *work?*

Our morphometric and physiological data are most consistent with the hypothesis that the book lungs and tracheae function in tandem, the lungs and tracheae serving the entire body and, in addition, the tracheae serving points of habitually great metabolic demand: the gonads and the nervous system (with that priority). The reasons for reaching this conclusion are the following.

A comparison of $\dot{V}_{O_2}$ and D_{O_2} values for small (group A) and large (group B) individuals gives ΔP_{O_2} values required to sustain mean metabolic rates for the entire respiratory system of between 0.72 and 0.86 kPa (Table 6). For an estimated peak $\dot{V}_{O_2}$ of 36 μl min^{-1} g^{-1}, a ΔP_{O_2} of 1.06–1.9 kPa is required. These values compare favourably with those for other, less-active species: on the basis of morphometric data, the estimated value for ΔP_{O_2} in *Tegenaria* spp. (Strazny and Perry, 1984) was 2.4 kPa for the maximum value of $\dot{V}_{O_2}$ measured during moulting. For the tarantula *Eurypelma californicum*, a ΔP_{O_2} of 7 kPa was measured across the walls of the lungs after activity, this value falling to 0.7 kPa during rest (Angersbach, 1978; Paul et al., 1987).

In *S. scenicus*, estimated peak $\dot{V}_{O_2}$ would result in ΔP_{O_2} values of 2.2–3.0 kPa for the lungs and 5.4–6.1 kPa for the tracheae (Table 6). As the tarantula has a better-developed circulatory system than that of jumping spiders, the ΔP_{O_2} values measured for the tarantula may be higher than can be achieved in *S. scenicus*. It is possible, therefore, that *S. scenicus* can only meet its maximal oxygen demands if the lungs and tracheae are working in parallel.

Looking separately at the two respiratory organs, the lungs or tracheae alone would suffice to supply the entire animal during resting and at low rates of activity at realistic ΔP_{O_2} levels, which all lie below 1.0 kPa (Table 6). Mean activity demands can also be met by the lungs alone (ΔP_{O_2}<1.4 kPa); however, the secondary tracheae on their own would need a ΔP_{O_2} of 2.4–2.7 kPa, which seems high in an animal in which the circulatory system is not well developed. In principle, the systems could, therefore, be used alternately during resting and low levels of activity. Since jumping spiders are observed to be active in full sunlight on warm days, it is possible that the tracheae may be a moisture-conserving supplement to lung breathing during periods of high metabolic activity at low humidity, thus allowing the lung spiracles to be only partly opened.

In general, the present study demonstrates that the tracheae contribute significantly to the total diffusing capacity of the respiratory system in jumping spiders. Tracheae have the advantage of high flexibility, being able to function as a combination of transport tubes and 'tracheal lungs'. Further studies of the lateral diffusing capacity of tracheal systems in arachnids will give insight into the functional anatomical flexibility that this mode of gas exchange provides.

We thank two anonymous referees that helped to improve a former version of the manuscript.

References

Anderson, J. F. (1970). Metabolic rates of spiders. *Comp. Biochem. Physiol.* **33**, 51–72.

Anderson, J. F. (1996). Metabolic rates of resting salticid and thomisid spiders. *J. Arachnol.* **24**, 129–134.

Anderson, J. F. and Prestwich, K. N. (1975). The fluid pressure pump of spiders (Chelicerata, Araneae). *Z. Morphol. D. Tiere* **81**, 257–277.

Anderson, J. F. and Prestwich, K. N. (1980). Scaling of subunit structures in book lungs of spiders (Araneae). *J. Morphol.* **165**, 167–174.

Anderson, J. F. and Prestwich, K. N. (1982). Respiratory gas exchange in spiders. *Physiol. Zool.* **55**, 72–90.

Anderson, J. F. and Prestwich, K. N. (1985). The physiology of exercise at and above maximal aerobic capacity in a theraphosid (tarantula) spider, *Brachypelma smithi. J. Comp. Physiol. B* **155**, 529–539.

Angersbach, D. (1978). Oxygen transport in the blood of the tarantula *Eurypelma californicum*: P_{O_2} and pH during rest, activity and recovery. *J. Comp. Physiol.* **123**, 113–125.

Baddeley, A. J., Gundersen, H. J. and Cruz-Orive, L. M. (1986). Estimation of surface area from vertical sections. *J. Microsc.* **142**, 259–276.

Bartels, H. (1971). Diffusion coefficients and Krogh's diffusion constants. In *Respiration and Circulation* (ed. P. L. Altman and D. S. Dittmer), pp. 21–22. *Biological Handbooks*. Bethesda, MA: Federation of American Societies for Experimental Biology.

Cruz-Orive, L. M. (1993). Systematic sampling in stereology. *Bull. Int. Statist. Inst. Proc.* **49**, 451–468.

Forster, R. R. (1980). Evolution of the tarsal organ, the respiratory system and the female genitalia in spiders. *Am. Mus. Nat. Hist.* **27**, 83–91.

Greenstone, M. H. and Bennett, A. F. (1980). Foraging strategy and metabolic rates in spiders. *Ecology* **61**, 1255–1259.

Gundersen, H. J. G. and Jensen, E. B. (1987). The efficiency of systematic sampling in stereology and its prediction. *J. Microsc.* **147**, 229–263.

Howard, C. V. and Reed, M. G. (1998). *Unbiased Stereology, Three-dimensional Measurement in Microscopy*. Oxford: Bios Scientific Publishers.

Krogh, A. (1919). The rate of diffusion of gases through animal tissues, with some remarks on the coefficient of invasion. *J. Physiol., Lond.* **52**, 391–408.

Levi, H. W. (1967). Adaptations of respiratory systems in spiders. *Evolution* **21**, 571–573.

Levi, H. W. (1976). On the evolution of tracheae in Arachnids. *Bull. Br. Arachnol. Soc.* **3**, 187–188.

Michel, R. P. and Cruz-Orive, L. M. (1988). Application of the Cavalieri principle and vertical sections method to lung: estimation of volume and pleural surface area. *J. Microsc.* **150**, 117–136.

Opell, B. D. (1987). The influence of web monitoring tactics on the tracheal system of spiders in the family Uloboridae (Arachnida, Araneae). *Zoomorphol.* **107**, 255–259.

Opell, B. D. (1990). The relationship of book lung and tracheal systems in the spider family Uloboridae. *J. Morphol.* **206**, 211–216.

Opell, B. D. (1998). The respiratory complementarity of spider book lung and tracheal systems. *J. Morphol.* **236**, 57–64.

Paul, R., Fincke, T. and Linzen, B. (1987). Respiration in the tarantula *Eurypelma californicum*: evidence for diffusion lungs. *J. Comp. Physiol. B* **157**, 209–217.

Perry, S. F. (1978). Quantitative anatomy of the lungs of the red-eared turtle, *Pseudemys scripta elegans*. *Respir. Physiol.* **35**, 245–262.

Perry, S. F. (1981). Morphometric analysis of pulmonary structure. Methods for evaluation and comparison of unicameral lungs. *Mikroskopie (Wien)* **38**, 278–293.

Perry, S. F., Hein, J. and van Dieken, E. (1994). Gas exchange morphometry

of the lungs of the tokay, *Gekko gecko* L. (Reptilia: Squamata: Gekkonidae). *J. Comp. Physiol. B* **164**, 206–214.

Prestwich, K. N. (1983). The roles of aerobic and anaerobic metabolism in active spiders. *Physiol. Zool.* **56**, 122–132.

Schmitz, A. and Perry, S. F. (1999). Stereological determination of tracheal volume and diffusing capacity of the tracheal walls in the stick insect *Carausius morosus* (Phasmatodea, Lonchodidae). *Physiol. Biochem. Zool.* **72**, 205–218.

Schmitz, A. and Perry, S. F. (2000). The respiratory system of Arachnids. I. Morphology of the respiratory system of *Salticus scenicus* and *Euophrys lanigera* (Arachnida, Araneae, Salticidae). *Arthr. Struct. Dev.* **29**, 3–12.

Strazny, F. and Perry, S. F. (1984). Morphometric diffusing capacity and functional anatomy of the book lungs in the spider *Tegenaria* spp. (Agelenidae). *J. Morphol*. **182**, 339–354.

Weibel, E. R. (1970/71). Morphometric estimation of pulmonary diffusion capacity. I. Model and method. *Respir. Physiol*. **11**, 54–75.

Weibel, E. R. and Knight, B. W. (1964). A morphometric study of the thickness of the pulmonary air–blood barrier. *J. Cell Biol.* **21**, 367–384.

Weygoldt, P. and Paulus, H. F. (1979). Untersuchungen zur Morphologie, Taxonomie und Phylogenie der Chelicerata. I. Morphologische Untersuchungen. *Z. Zool. Syst. Evolut.-Forsch*. **17**, 85–115.